Luminescent Erbium-Doped Porous Silicon Bilayer Structures**

By *Lanlan Gu*, *Zuhong Xiong*, *Gang Chen*, *Zhisong Xiao*, *Daiwei Gong*, *Xiaoyuan Hou*, and *Xun Wang**

In recent years, the optical properties of erbium-doped silicon (Si:Er) have attracted much attention due to the potential use of Si:Er in opto–electronic devices integrated with established silicon technology.[1] The emission at approximately 1.54 μm from the intra-4f shell transition of erbium is of considerable interest, since it coincides with the window of maximum transmission for silica-based optical fibers. However, the temperature quenching of the luminescence due to the energy back-transfer from the erbium ions to the silicon host is a formidable obstacle that prevents practical applications of Si:Er materials. Porous silicon (PSi) is a promising candidate for replacing silicon as the host material. Among other things, the bandgap of PSi (>1.5 eV) is wider than that of silicon. The energy back-transfer (de-excitation) process would be less efficient, and thus the temperature quenching of the erbium-related luminescence would be less serious.[2,3] To date, erbium has been introduced into porous silicon through electrochemical deposition,[3,4] ion implantation,[5–7] spin-on,[8,9] and immersion[10,11] techniques. However, in all of these cases, the incorporation of erbium was carried out after the formation of PSi. It is thus hard to identify whether the erbium atoms are located inside the nanostructures, or just attached to the inner surfaces of the pores: leading to some argument about the sites of the Er^{3+} luminescent centers.[11,12] Furthermore, in order to remove implantation damage, or to introduce oxygen into the PSi matrix in order to activate the Er^{3+} centers, a high-temperature annealing process is required, and this appears to be disadvantageous to the PSi matrix.

In this work, we present a novel approach to preparing PSi:Er, i.e., the anodization of an erbium and oxygen co-doped silicon layer grown by molecular beam epitaxy (MBE). A unique characteristic of this method is that it ensures a uniform distribution of erbium ions in the PSi, as a function of depth, for any epitaxial thickness. High-temperature annealing is thus not necessary, as the co-doping of oxygen and erbium is achieved during the MBE growth. A reasonably narrow photoluminescence (PL) peak at ~1.54 μm was observed at room temperature, without employing any post-treatment. Moreover, this approach offers the opportunity for making a direct comparison between the PL behavior of erbium in sili-

con both before and after anodization. This is informative, and helps to clarify the role played by PSi as the host matrix. From comparisons of the morphologies and PL of PSi:Er and PSi etched under the same conditions, the earlier understanding—that when erbium is doped in silicon it behaves as a donor impurity—was verified.

The growth of erbium oxygen co-doped silicon epilayers was carried out at a growth temperature of 500 °C by MBE on a p-type Si(100) substrate. The reflection high energy electron diffraction (RHEED) spots showed that the epilayer is actually crystalline, and in excellent registry with the substrate. The thickness of the epilayer used in the samples described in this paper was 500 nm. After the sample was taken out of the vacuum chamber, it was cut into pieces and then anodized in an $HF/C_2H_5OH/H_2O$ = 1:1:2 electrolyte solution. The anodization was carried out in the dark, at anodic currents of 5 and 30 mA/cm^2. For comparison, Si(100) wafers without erbium dopant were also treated under the same conditions. A series of samples of PSi:Er and PSi fabricated under different etching conditions are listed in Table 1. Series A is PSi:Er; series B is PSi anodically etched on a p-Si(100) wafer with a resistivity of 5–8 Ω cm; series C is PSi anodically etched on a n-Si(100) wafer with a resistivity of 10–14 Ω cm.

Table 1. The etching conditions of PSi:Er and PSi samples.

Sample	Material	Current density [mA/cm^2]	Time [min]
A1	PSi:Er	5	10
A2	PSi:Er	30	5
A3	PSi:Er	5	5
A4	PSi:Er	30	3
B1	p-PSi	5	10
B2	p-PSi	30	5
C1	n-PSi	5	10
C2	n-PSi	30	5

The PL spectra of the samples were measured using the 441.6 nm line of a He-Cd laser as the excitation source. The signals were amplified by standard lock-in techniques, and detected by a photomultiplier in the visible region, and by a liquid nitrogen cooled Ge detector in the infrared region. The morphologies of the samples were observed by scanning electron microscopy (SEM). Rutherford backscattering (RBS) was employed to detect the erbium content in the samples quantitatively. The ratios of erbium to silicon extracted from the RBS spectra of the PSi:Er and Si:Er samples demonstrate that the Er/Si ratio remains unchanged after anodization, which implies that the remaining erbium atoms in the PSi:Er sample are most likely inside the silicon nanostructures.

The surface morphologies of the PSi:Er and PSi samples are shown in Figure 1. The p-PSi sample (B2) and the n-PSi sample (C2) have fairly different surface morphologies. The evident cracks and islands, which are surrounded by many extremely small pinholes on B2, are representative of the morphology of PSi on a lightly doped p-type substrate.[13–15] The piping surface shown on sample C2 is characteristic of the mor-

[*] Prof. X. Wang, L. Gu, Dr. Z. Xiong, G. Chen, Dr. D. Gong, Prof. X. Hou
Surface Physics Laboratory, Fudan University
Shanghai 200433 (China)
E-mail: xunwang@fudan.ac.cn
Z. Xiao
Institute of Low Energy Nuclear Physics
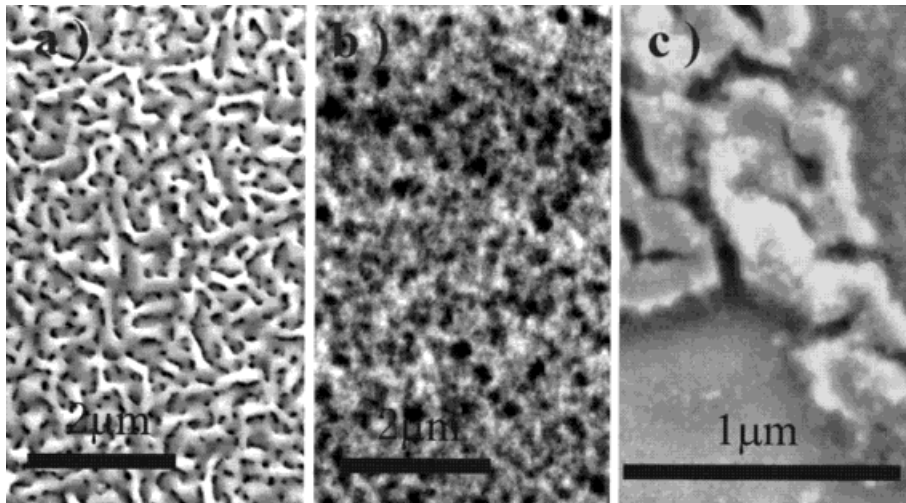Beijing Normal University
Beijing 100875 (China)

Fig. 1. SEM plane views of PSi:Er and PSi samples. a) PSi:Er sample, A2. b) n-PSi sample, C2. c) p-PSi sample, B2.

phology of n-type PSi. The uniform honeycomb-like surface of PSi:Er (A2) is rather similar to that of n-PSi (C2). Generally, the pore diameters in n-type silicon are considerably larger than those in p-type silicon, and they show a strong tendency to form straight channels (sometimes called trenches) at low dopant concentration.[14] The sharp contrast between the trench-like top layer and the filament-like layer underneath, observed on the image of A2 at a viewing angle of 40° (Fig. 2), indicates that the erbium doped in silicon (via MBE) acts as a

donor rather than an acceptor. Such donor-like behavior of erbium in silicon has been demonstrated by previous C–V measurements.[16–18] We also performed C–V measurements of our erbium-doped silicon epitaxial layers, since the Er-doped silicon layers were grown on top of a silicon buffer layer in MBE. We found that the unintentionally doped silicon epilayer was usually p-type. Thus, the test structure is a (p-type)Si cap/ Er-doped (n-type)Si/(p-type)Si buffer/(p-type)Si substrate. Such a structure will give rise to abnormal C–V characteristics. By numerically solving the Poisson equation in a Schottky contact/p-n-p potential barrier, the carrier type of the Er-doped silicon layer was verified as being electron conduction.[19] Further evidence in support of the donor behavior of erbium in silicon will be described below.

Cross sectional SEM (XSEM) images of samples A1 and A2 are shown in Figure 2. The images show that the etched layers of both of these samples are more substantial than the etched Si:Er epilayer. The anodization was extended into the substrate by about 500 nm for samples A1 and A2. Samples A3 and A4 were fabricated with shorter etching times (about half that of samples A1 and A2), which limited the pore formation within the Si:Er epilayers.

Figure 3 shows the visible PL spectra at room temperature of a) PSi:Er and b) PSi samples. The PL peaks of samples A1
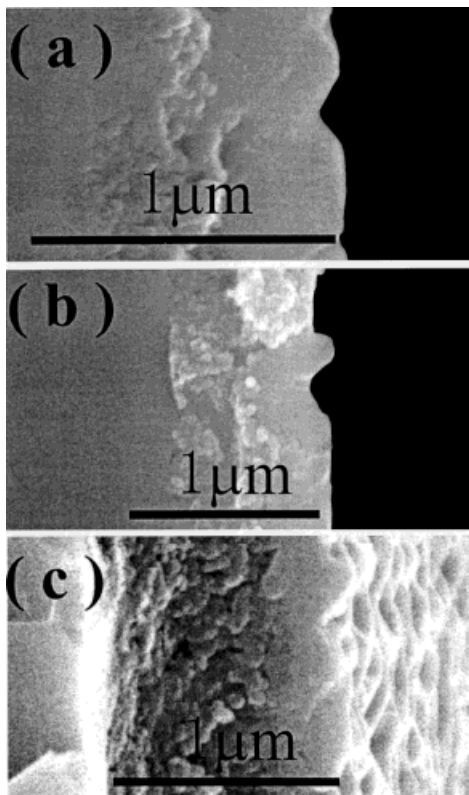

Fig. 2. Cross sectional SEM micrographs of PSi:Er. a) Sample A1; b) sample A2; c) sample A2 at a viewing angle of 40°.
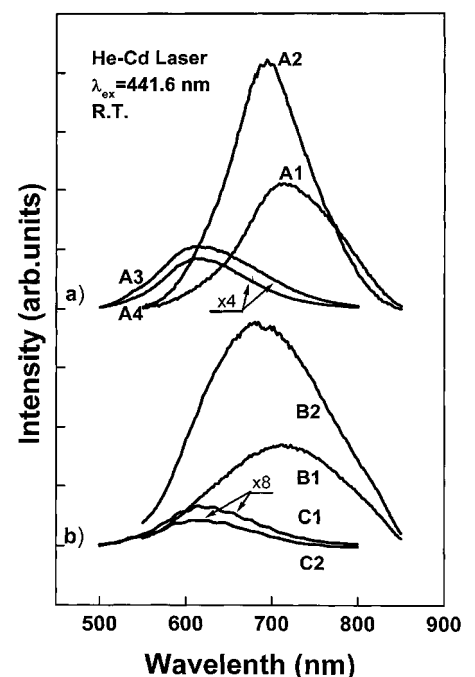

Fig. 3. PL spectra of PSi:Er samples at room temperature. a) p-PSi samples. b) n-PSi samples.

and A2 are centered near 700 nm, whereas those of A3 and A4 are centered at higher energy (near 610 nm). Comparing the PL spectra of all the samples (Fig. 3), we note that the peak positions of A3 and A4 coincide with those of n-PSi (i.e., samples C1 and C2), and the peak positions of A1 and A2 coincide with those of the p-PSi samples (i.e., samples B1 and B2). Since the XSEM images indicate that the PSi layers of A3 and A4 are limited in the Er-doped epilayer, the PL peaks of these samples must have originated from the PSi:Er film. The similarity between the PL spectra of A3 and A4, and those of C1 and C2, provides another piece of indirect evidence showing that the erbium in silicon behaves like a donor impurity. With regard to samples A1 and A2: since the etched layers of these samples are much thicker than those of the Er-doped epilayers, the PL originating from both the etched substrate and the etched Er-doped epilayer contributes to the spectra. However, since the visible peak from the n-like PSi:Er layer is much weaker than that from the p-PSi substrate, and the luminescence could penetrate through the PSi:Er layer without noticeable attenuation, the overall PL spectra look more like that of p-PSi.

Figure 4 shows the infrared PL spectra of PSi:Er measured at 80 K. The visible PL spectra at 80 K are similar to those observed at room temperature. There are some correlations
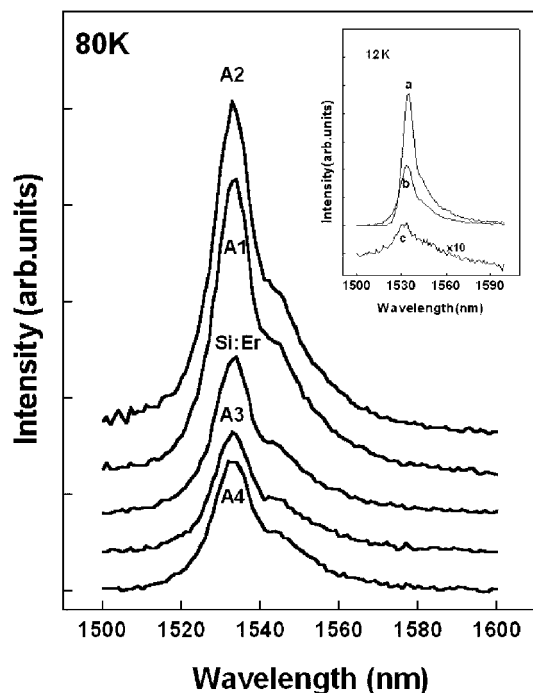

Fig. 4. PL spectra of samples A1, A2, A3, and A4, in the infrared region (at 80 K). The inset shows the PL spectra (at 12 K) of a) PSi:Er, b) Si:Er, and c) erbium-implanted silicon oxide film.

between the visible luminescence band and the infrared PL peak. Samples A1 and A2, both of which have an intense luminescence in the visible region near 700 nm (~1.7 eV), exhibit a prominent enhancement of the light at ~1.54 μm. For samples A3 and A4, both of which have their visible

absorbance shifted to shorter wavelength (near 600 nm; ~2.0 eV), the magnitude of the infrared PL is about a factor of 2 smaller than the PL of samples A1 and A2. This change in the luminescence intensity at ~1.54 μm, versus that of the visible band, follows the same trend as that observed by Kimura et al.[4] This observation further supports the opinion that the excitation of Er^{3+} in PSi occurs via an energy transfer process that takes place after the recombination of the electron–hole pairs (that are confined in the nanostructures). Since the energy difference between the erbium intra-4f levels $^4I_{9/2} \rightarrow {}^4I_{15/2}$ is about 1.55 eV, which is considered to be the pump energy of Er^{3+} in PSi, the apparent energy bandgap of 1.7 eV inferred from the PL centered near 700 nm is closer to this value than to 2.0 eV (600 nm). It is more likely that samples A1 and A2 would undergo this efficient excitation. From the previous argument that the intense visible luminescence centered near 700 nm of A1 and A2 is radiated from the PSi layer beneath the PSi:Er, it is reasonable to deduce that the energy transfer performed by photocarriers is available, even though the erbium ions are physically separated from the regions where carrier generation and recombination processes occur. This is in agreement with the conclusion made by Shin et al.[20] Therefore, we suggest the following luminescence mechanism for our A1 and A2 samples: i) the excitation of photocarriers occurs primarily in the underlying PSi layer; ii) the energy is transferred to the erbium centers in the top PSi:Er layer above the PSi; and iii) the intra-4f transition of erbium gives rise to the 1.54 μm luminescence. Because the apparent energy gap of PSi:Er (2.0 eV) is much larger than 0.8 eV (corresponding to 1.54 μm), the energy back-transfer process in the top PSi:Er layer may be greatly suppressed. The efficient excitation and the suppressed energy back-transfer in this mechanism take advantage of the modulated bandgap of the PSi(Er)/PSi bilayer. This can be only achieved by MBE. We believe that by optimizing the thicknesses and porosities of the top PSi:Er layer and the PSi layer underneath (as well as the erbium, oxygen, and other dopant concentrations) the luminescence properties of this kind of sample can be further improved.

The inset of Figure 4 shows the infrared PL spectra of Er-doped silicon samples before and after anodization under a current density of 30 mA/cm² for 5 min. Although anodization removes at least 70 % of the erbium, the PL intensity is enhanced by more than a factor of two, indicating the effectiveness of using PSi as a host matrix. The peak width of 6 nm (FWHM) at 12 K does not change after anodization, and this implies that the erbium distribution in the nanostructures is uniform. By using ordinary preparation methods, the peak width of PSi:Er is generally broader than 10 nm at 12 K.[4,5,21]

For comparison, the inset of Figure 4 also shows the PL spectrum of an erbium-implanted oxidized silicon sample. This sample was prepared by ion implantation of erbium into a silicon oxide film. Although the peak erbium concentration in this sample (determined by RBS) is about 100 times higher than that in our sample, its PL intensity is weaker than that of our sample by a factor of about 40.

In conclusion, a novel method for preparing luminescent Er-doped PSi—by anodically etching an MBE grown Si:Er epilayer—has been presented. A reasonably narrow PL peak at 1.54 μm was obtained, implying a highly uniform distribution of erbium in the host matrix. We propose that photocarriers excited in the PSi layer transfer their energy to the erbium ions in the top PSi:Er layer, and the energy back-transfer process, which occurs by carrier recombination, is greatly suppressed due to the large bandgap of PSi:Er. It is possible to achieve high efficiency PL by such a PSi:Er/PSi double layer if the structural, compositional, and etching parameters are optimized. The comparisons of the surface morphologies and the PL peak positions between the PSi:Er, n-PSi, and p-PSi samples provide indirect evidence for the donor-like behavior of erbium doped in silicon.

[1] S. Coffa, G. Franzo, F. Priolo, *Mater. Res. Soc. Bull.* **1998**, *23(4)*, 25.
[2] U. Hommerich, F. Namavar, A. M. Cremins-Costa, K. L. Bray, *Appl. Phys. Lett.* **1996**, *68*, 1951.
[3] T. Dejima, R. Saito, S. Yugo, H. Isshiki, T. Kimura, *Appl. Phys. Lett.* **1998**, *84*, 1036.
[4] T. Kimura, A. Yokoi, H. Horiguchi, R. Saito, T. Ikoma, A. Sato, *Appl. Phys. Lett.* **1994**, *65*, 983.
[5] F. Namavar, F. Lu, C. H. Perry, A. Cremins, N. M. Kalkhoran, R. A. Scoref, *J. Appl. Phys.* **1995**, *77*, 4813.
[6] J. H. Shin, G. N. Van den Hoven, A. Polman, *Appl. Phys. Lett.* **1995**, *66*, 2379.
[7] T. Taskin, S. Gardelis, J. H. Evans, B. Hamilton, A. R. Peaker, *Electron. Lett.* **1995**, *31*, 2132.
[8] A. M. Dorofeev, N. V. Gaponenko, V. P. Bondarenko, E. E. Bachilo, N. M. Kazuchits, A. A. Leshok, G. N. Troyanova, N. N. Vorosov, V. E. Borisenko, H. Gnaser, W. Bock, P. Becker, H. Oechsner, *J. Appl. Phys.* **1995**, *77*, 2679.
[9] A. Dorofeev, E. Bachilo, V. Bondarenko, N. Gaponenko, N. Kazuchits, A. Leshok, G. Troyanova, N. Vorozov, V. Borisenko, H. Gnaser, W. Bock, P. Becker, H. Oechsner, *Thin Solid Films* **1996**, *276*, 171.
[10] X. Zhao, S. Komuro, H. Isshiki, S. Maruyama, Y. Aoyagi, T. Sugano, *Appl. Surf. Sci.* **1997**, *113/114*, 121.
[11] W. Wang, H. Isshiki, S. Yugo, R. Saito, T. Kimura, *J. Lumin.* **2000**, *87–89*, 319.
[12] M. Stepikhova, L. Palmetshofer, W. Jantsch, H. J. von Bardeleben, *Appl. Phys. Lett.* **1999**, *74*, 537.
[13] C. Lin, S. Lee, Y. F. Chen, *J. Appl. Phys.* **1994**, *75*, 7728.
[14] R. L. Smith, S. D. Collins, *J. Appl. Phys.* **1992**, *71*, R1.
[15] A. G. Cullis, L. T. Canham, P. D. J. Calcott, *J. Appl. Phys.* **1997**, *82*, 909.
[16] J. L. Benton, J. Michel, L. C. Kimerling, D. C. Jacobson, Y. H. Xie, D. J. Eaglesham, E. A. Fitzgerald, J. M. Poate, *J. Appl. Phys.* **1991**, *70*, 2667.
[17] S. Libertine, S. Coffa, G. Franzo, F. Priolo, *J. Appl. Phys.* **1995**, *78*, 3868.
[18] V. V. Emtsev, V. V. Emtsev, Jr., D. S. Poloskin, E. I. Shek, N. A. Sobolev, J. Michel, L. C. Kimerling, *Physica B* **1999**, *273–274*, 346.
[19] F. Lu, personal communication.
[20] J. H. Shin, W.-H. Lee, H.-S. Han, *Appl. Phys. Lett.* **1999**, *74*, 1573.
[21] X. Wu, U. Hommerich, *Appl. Phys. Lett.* **1996**, *69*, 1903.